Estimation of Critical Carbon Particle Engulfment Velocity in Metallurgical Melts

S.K. Khanna, C. Wu and V. Sahajwalla

School of Materials Science and Engineering,
The University of New South Wales,
Sydney, NSW 2052, Australia

(Received January 12, 1998)

ABSTRACT

The critical velocity of engulfing carbon particles in metallurgical melts controls the interfacial area available for the carbon/melts reaction and subsequently dictates the overall pyrometallurgical process. Because of difficulty with high temperature experiments, the relationship of the engulfment velocity and forces acting on the carbon particles has not been well established. In this study, a model based on the principle of force balance and equation of motion has been proposed to estimate the critical carbon particle engulfment velocity for high temperature metallurgical systems. The present model improves upon the existing expressions by including a precise treatment of buoyancy force on particles. The computed results were validated against the experimental data on injection of spheres (glass, stainless steel, sapphire and Hastelloy B) into a mercury bath and were found to be in excellent agreement. The critical engulfment velocities for coal/slag systems were estimated by taking into account the measured carbon/slag interfacial contact angle. The results were found to lie in between the proposed penetration velocity obtained by using Siderenko correlation and that obtained by using Voronova correlation.

Using this model for carbon/slag systems (CaO-SiO_2-Al_2O_3-MgO-Fe_2O_3), the critical carbon particle engulfment velocities were found to range from 4.3 to 5.6 m/s for particles 100 μm in size. In carbon/Fe-C-S systems, for particles about 100 μm in size, this value ranged from 2.4 m/s to 7.2 m/s. The critical particle engulfment velocity was estimated as a function of particle size and interfacial contact angle characterising the wettability at the carbon/melt interface. An increase in carbon content of the melt lead to increased values of contact angles and of critical engulfment velocities. Due to poor wettability, engulfment of carbon particles of the same size will be more difficult in melts containing higher carbon levels. It is concluded that for the carbon particles typically employed in metallurgical processes, the wettability between particles and melts has a significant influence on the critical engulfment velocity and therefore could dictate the carbon/melt interfacial area and any subsequent reactions occurring at the interface.

KEY WORDS

Engulfment velocity; contact angle; wettability; slag; melts.

1. INTRODUCTION

The injection of solid particles into metallurgical melts is an essential step in preparing low cost, high quality steels and in non-ferrous pyrometallurgical applications. Some processes utilise an inert gas carrier to add granular or powdered materials to the melt through a lance and this is found to enhance reaction rates and refinement efficiencies /1/. In the emerging direct iron smelting technologies, carbonaceous particles are injected either into the slag phase or into the metal

phase. The purpose is ultimately to achieve reduction of iron oxide in the slag phase, which is dependent on the slag/carbon and metal/carbon interfacial phenomena /2/. The critical velocity of injection of carbon particles which will lead to engulfinent has a significant bearing on the process, since it will dictate the interfacial area available for the carbon/melt reaction. The critical velocity is expected to be dependent on forces at the solid/liquid interface. This could not be taken into account accurately while estimating critical velocities in high temperature melts due to lack of data on interfacial contact angles.

Melt/carbon contact is also important in other significant areas such as pulverised coal injection in blast furnaces. Although coal is injected into the gas phase through the tuyeres, the unburnt char particles enter the blast furnace burden and interact with the liquid phases, metal and slag /3/. Once again, the critical velocity for particle engulfinent by the melt phases has a significant bearing on the process, since the assimilation of the unburnt char by the melt has a strong influence on the blast furnace permeability which is dictated by interaction area.

Although many published expressions could be used to predict critical engulfinent velocity in different systems, a model with a precise mathematical representation of the particle buoyancy force is still not available. The present model comprehensively takes into account the influence of different forces and is expected to yield more accurate estimates of the critical particle engulfinent velocity.

2. PREVIOUS STUDIES

Most of the models used to predict the engulfinent velocity for gas/liquid surfaces require a Weber number correlation *We*, which is defined as:

$$We = \frac{\rho_l r_p v_c^2}{\gamma_{lv}} \qquad (1)$$

where ρ_l is the density of liquid, v_c is the critical entry velocity for particle penetration, γ_{lv} is gas/liquid surface tension and r_p is the particle radius. However, the correlation could vary over a wide range. The maximum correlation, as derived by Siderenko /4/, can be expressed as:

$$We = 10.91(2 + \frac{0.5}{\rho^*})\left[\exp(0.55\rho^*) - 1\right] \qquad (2)$$

Here ρ^* is the ratio of the density of the particle and liquid. The minimum correlation was derived by Voronova /5/ as:

$$We = \frac{3}{\rho^*} \qquad (3)$$

Jorgensen *et al.* /6/ calculated maximum and minimum critical coal particle penetration velocities at the gas/slag interface by using Siderenko and Voronova's correlations. The critical velocity was found to vary over a wide range for particle sizes ranging from 1 μm to 100 μm. The maximum velocity was 153 m/s for the minimum particle size (1 μm) and the minimum velocity of 4 m/s corresponded to a maximum particle size of 100 μm. All these velocities were found to be well below the lance exit velocity used in the injection system. These results indicate that the majority of the goal particles will probably penetrate the gas envelope and pass into the slag.

Engh *et al.* /7/ used an equation of motion to calculate the critical size of the particle that can penetrate the argon bubble steel melt interface. In their approach, the inertial force was assumed to be equal to the sum of the drag force of melt on the particle and the surface tension force. The force acting on the particle due to surface tension was taken into account by obtaining total surface energy as a function of penetration depth.

Ozawa and Mori /8/ have experimentally studied the behaviour of a sphere penetrating into mercury and developed an expression for critical velocity based on the equation of motion and force balance. The buoyancy force and the force due to gravity were included in this study, in addition to the drag force and the surface tension force. The buoyancy force acting on the sphere changes with the penetration depth of the sphere. However, Ozawa and Mori equated it to the force acting on a half immersed sphere. No reason was offered for this assumption. The critical Weber number was expressed as:

$$We = \frac{4A}{C_D}\left\{\left(1-\exp\left(\frac{3C_D}{2\rho^* + 0.25}\right)\right)\left(\frac{4(\rho^* + 0.25)}{3C_D} - 1 + \cos\theta + \frac{2G(\rho^* - 0.5)}{3A}\right) + 2\right\} \quad (4)$$

where A is an empirical constant, C_D is the drag coefficient, θ is the contact angle and G is a dimensionless constant representing the relation between the buoyancy force and surface tension force.

$$G = \frac{r_p^2 \rho_l g}{\gamma_{lv}} \quad (5)$$

The computed Weber numbers were in reasonable agreement with the experimental data on critical entry velocity. However, the treatment of buoyancy force in this model is only approximate and the effect of penetration depth on the buoyancy force has not been properly accounted for. Therefore, it is important to develop a new model taking into account the exact contribution of the buoyancy force to the overall force balance and to make an accurate prediction of the engulfment velocity from an equation of motion.

3. THEORETICAL MODEL

Fig. 1 gives a schematic representation of a sphere entering a melt. Using an equation of motion, the total force F_{tot} acting on this sphere can be written as:

$$F_{tot} = -\frac{4}{3}\pi r_p^3 \left(\rho_p + \rho_l \alpha\right)\frac{dv}{dt} \quad (6)$$

where ρ_p is the density of the particle, ρ_l is the density of the melt, r_p is the particle radius, v is the particle velocity, and $-\frac{dv}{dt}$ represents its deceleration, α is the virtual mass coefficient which accounts for that part of the liquid which moves with the spherical particle.

The total force acting on a moving spherical particle is composed of four parts:

$$F_{tot} = F_G + F_S + F_B + F_D \quad (7)$$

(1) Gravitational force, F_G, depends only on the physical mass of the particle and is independent of particle motion and its position in the liquid. F_G can be written as:

$$F_G = \frac{4}{3}\pi r_p^3 \rho_p g \quad (8)$$

(2) The force, F_S arising due to surface tension at the liquid-solid interface can be expressed as /8/:

$$F_S = 2\pi r_p \gamma_{lv} A\left(\frac{x}{r_p} - 1 - \cos\theta\right) \quad (9)$$

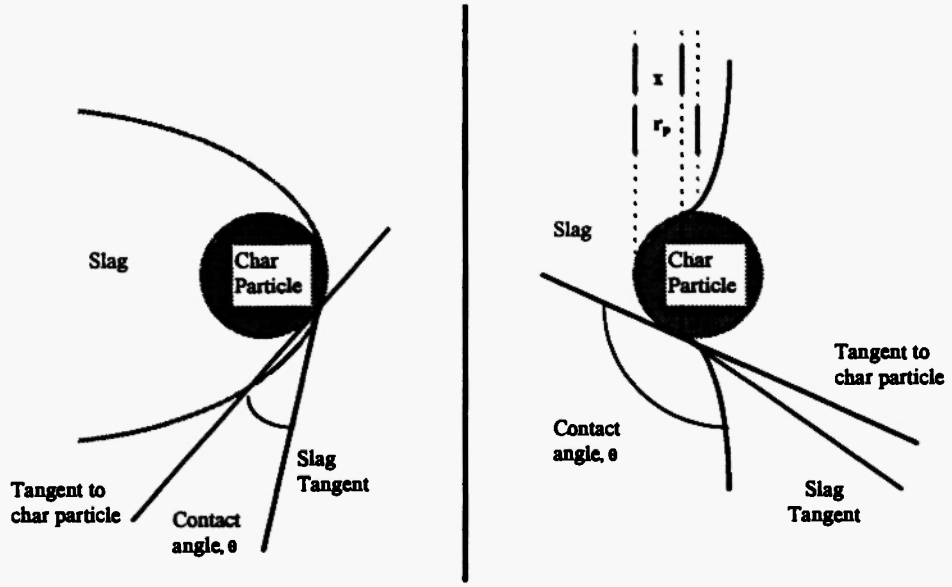

Fig. 1: Schematic representation of a char particle in contact with molten slag, (a) good wetting, $\theta < 90°$, (b) poor wetting, $\theta > 90°$. r_p is the particle radius and x represents the penetration depth.

where γ_{lv} is the gas-melt interfacial tension, x is the penetration depth, θ is the contact angle, A is the correction factor which accounts for an increase in the surface tension force due to cavity formation when the sphere impinges on the surface of the liquid.

(3) Buoyancy force, F_B, acts on the immersed part of a spherical particle and changes with the penetration depth x of the spherical particle in liquid. F_B can be written as:

$$F_B = \frac{1}{3}\pi\left(3r_p x^2 - x^3\right)\rho_l g \tag{10}$$

(4) Drag force, F_D, due to fluid motion can be described as:

$$F_D = \frac{1}{2}\pi r_p^2 \rho_l v^2 C_D \Phi\left(x/r_p\right) \tag{11}$$

where C_D is the drag coefficient and v, typically, will be of the order of the characteristic velocity in the liquid. $\Phi(x/r_p)$ is a correction factor for C_D and it varies with penetration depth. Its value will be 1 when the sphere is perfectly immersed. The value of the drag coefficient C_D has been taken as 0.44 as suggested by Bird *et al.* /9/.

The forces on the particle due to surface tension, buoyancy, and drag are all repulsive in nature and will have a positive value. The force due to gravity is always attractive and therefore has a negative value. At equilibrium, a force balance for the particle in a direction normal to the solid/liquid interface will yield the following equation of motion:

$$-\left(\frac{4}{3}\right)\pi r_p^3\left(\rho_p + \rho_l\alpha\right)\frac{dv}{dt} = \frac{1}{3}\pi\left(3r_p x^2 - x^3\right)\rho_l g - \frac{4}{3}\pi r_p^3 \rho_p g + 2\pi r_p \gamma_{lv} A\left(\frac{x}{r_p} - 1 - \cos\theta\right) + \frac{1}{2}\pi r_p^2 \rho_l v^2 C_D \Phi\left(x/r_p\right) \tag{12}$$

When a sphere just comes into contact with the liquid surface, its virtual mass will be zero. If the sphere is completely immersed in the liquid, its virtual mass is equal to the mass of the liquid displaced by the sphere /10/. The virtual mass coefficient α is expected to take a value between 0 and 0.5 according to the penetration depth of the sphere. Assuming that the virtual mass is equal to half of the mass of the liquid displaced by a half-immersed sphere /8/, α can be taken to be 0.25.

Equation (12) can be rewritten as

$$\frac{v^2}{a} + \frac{b}{a}f(x) + \frac{1}{2}\frac{dv^2}{dx} = 0 \tag{13}$$

where a, b and $f(x)$ are defined as

$$a = \frac{8r_p\left(\rho^* + 0.25\right)}{3C_D} \tag{14}$$

$$b = \frac{4\gamma_{lv}A}{r_p\rho_l C_D} \tag{15}$$

$$f(x) = \left(\frac{x}{r_p} - 1 - \cos\theta\right) - \frac{ag\rho^*}{b\left(\rho^* + 0.25\right)} + \frac{ga\left(3r_p x^2 - x^3\right)}{4br_p^3\left(\rho^* + 0.25\right)} \tag{16}$$

The solution of the differential equation (13) can be written as

$$v^2 = \exp\left(\frac{-2}{a}\int_0^x dx\right)\left[v_0^2 - \left(\frac{2b}{a}\right)\int_0^x f(x)\exp\left(\frac{2}{a}\int_0^x dx\right)dx\right] \tag{17}$$

where v_0 is the initial velocity of the particle relative to the interface. A negative right hand side in equation (17) will lead to an imaginary value of v. The condition for penetration therefore requires the right-hand side of equation (17) to remain positive for $x = 2r_p$. The solution of equation (17) thus yields an expression for the critical velocity v_c

$$v_c^2 = b\left[\left\{\left(1 + \frac{ac}{2}\right)\left(1 - \frac{a}{2r}\right) - \cos\theta - \frac{ag\rho^*}{b\left(\rho^* + 0.25\right)}\right\}\left(e^{\frac{4r_p}{a}} - 1\right) + 2 - \frac{4r_p^2 c}{3a}e^{\frac{4r_p}{a}} + ac\right] \tag{18}$$

where

$$c = \frac{3a^2 g}{4br_p^2\left(\rho^* + 0.25\right)} \tag{19}$$

4. RESULTS AND DISCUSSION

4.1. Validation of New Model with Available Experimental Data

The critical velocities for engulfment of glass, stainless steel, sapphire and Hastelloy B spheres into a mercury bath were calculated using equation (18) and the available values of θ, ρ^*, γ_{lv}, and A. The computed results as a function of the particle size are shown in Figure 2 and were found to be in excellent agreement with previous experimental results. The critical velocities calculated from equation (18) were also compared with those derived from the relations developed

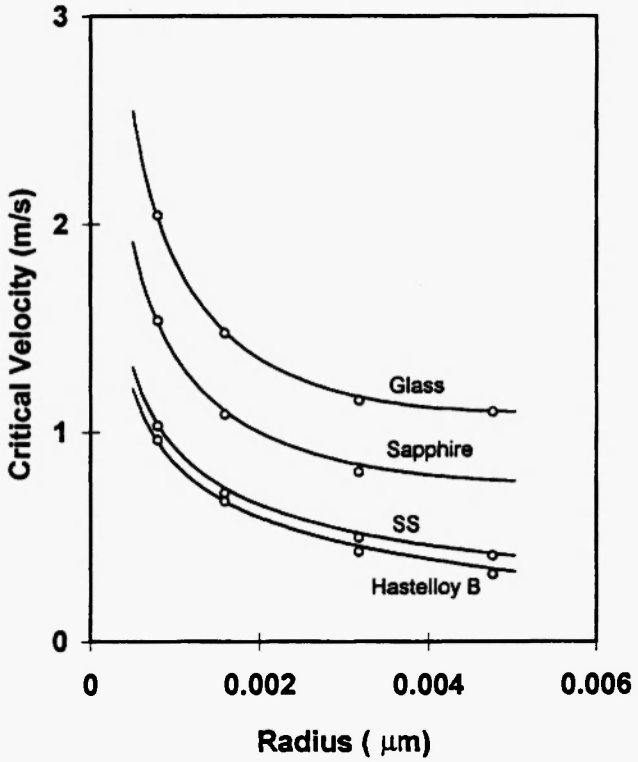

Fig. 2: Comparison of calculated critical velocities of glass, stainless steel, sapphire and Hastelloy B (shown as solid lines) with experimental data on critical velocities.

by Siderenko and Voronova (equations 2 and 3). The relations given by Siderenko and Voronova were used by Jorgensen *et al.* /6/ to predict the maximum and the minimnm critical penetration velocities for coal/slag systems. These values are independent of the interfacial phenomena. A set of three reasonable contact angles θ (100°, 110 and 120°) in the same coal/slag system were selected to evaluate the critical entry velocity. Using identical values of the parameters (γ_{lv}, ρ_p and ρ_l), the critical engulfment velocities were calculated and have been plotted in Figure 3 along with Jorgensen's results. The computed results lie in between those calculated from the correlations of Siderenko and Voronova, but are closer to those of Voronova.

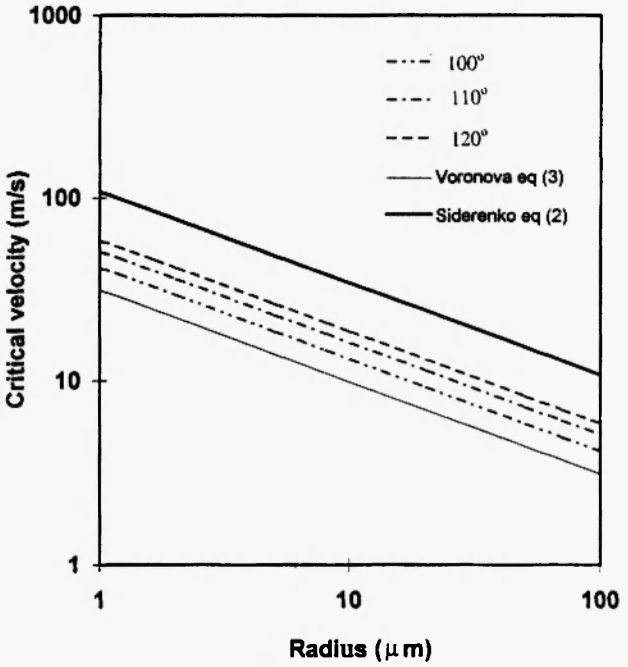

Fig. 3: Effect of particle size on critical velocities in coal/slag system for different contact angles. Correlations due to Voronova /5/ and siderenko /4/ are also shown in the figure.

4.2. The Critical Velocity of Engulfment for Carbon/Slag Systems

The critical engulfment velocities for carbon particles in iron smelting slags were evaluated using equation (18). The contact angle between carbon and slag was measured using a sessile drop method. The slag composition and corresponding contact angles are given in Table 1.

Typical carbon particle size employed for injection of coal into molten slag ranges from 10 to 100 μm. The slag density and surface tension used in the calculation of the critical velocity are ρ_l = 2800 kg/m^3 and γ_{lv} = 0.46

Table 1
Slag composition and measured contact angles /2/

Slag	Al_2O_3	CaO	MgO	SiO_2	Fe_2O_3	θ
1	23.8	37.7	5.19	33	0.21	123°
2	24	47.3	0.11	28.1	0.22	107°
3	21.5	47.5	0.14	28.6	2.15	105°

Nm /11/. The density of solid carbon particle employed is ρ_p = 1600 kg/m^3. Figure 4 shows a plot of critical velocity as a function of particle size for different slags. It is observed that the critical engulfment velocities for the above set of slags show a similar dependence on particle size. The value of critical velocity for a 100 μm carbon particle lies between 4.3 to 5.6 m/s.

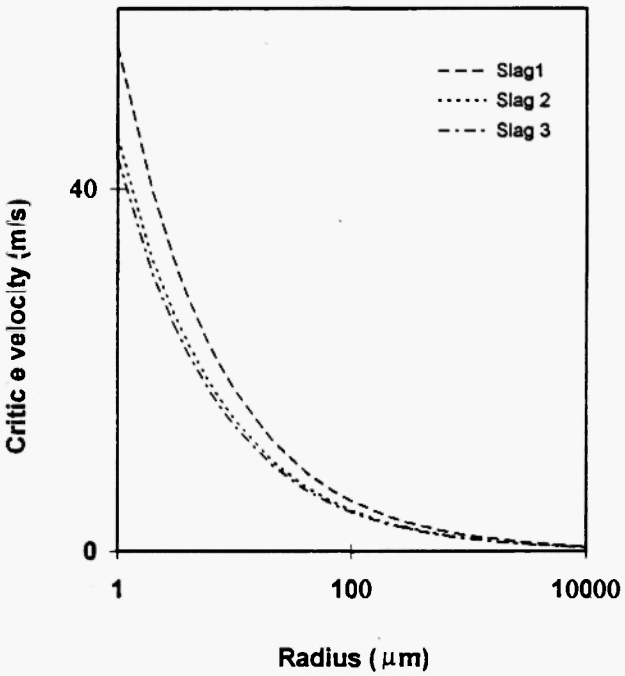

Fig. 4: Effect of particle size on critical engulfment velocities of carbon particle in Ca-MgO-SiO_2-Al_2O_3-Fe_2O_3 slags as a function of contact angle.

4.3. The Critical Velocity of Engulfment for Graphite/Fe-C-S Systems

The critical velocity of engulfment for graphite and Fe-C-S systems has been estimated using equation (18). Data on contact angles was obtained by the sessile drop method. The contact angles along with the corresponding melt carbon and sulfur concentrations are given in Table 2.

Table 2
Fe-C-S composition and measured contact angles

Carbon (wt%)	Sulfur (wt%)	θ
1.01	0.02	81°
2.0	0.02	87°
2.0	1.26	105°
2.0	2.36	118°

The interfacial tension of the melt surface was calculated using the equation proposed by Jimbo *et al.* /12/

$$\gamma_{lv} = 2184 - 0.107T \ln(1 + K_s a_s) \quad (20)$$

where T (= 1873K) represents the experimental temperature; a_s is the sulfur activity. It can be calculated according to melt sulfur and carbon content. The coefficient K_s is a function of temperature. The density for Fe-C-S melts is ρ_l = 6920.9 kg/m^3 /12/. The sensitivity tests were conducted on the effect of melt density on the calculated critical velocity. There was no significant effect of density on the critical velocity as a change in melt density by 3% leads to a change of 0.03% in the calculated values of critical velocity for these samples.

The critical velocities for the carbon/Fe-C-S systems as a function of particle size are plotted in Figure 5. The critical velocity of the particle increases with decreasing carbon particle size. However, for a fixed particle size, the critical velocity was seen to increase with contact angle (Figure 6). The engulfment velocity of a carbon particle of size 100 μm is found to be 7.2 m/s in Fe-C (2%) – S (2.36%) melt and for a particle of size 10 μm, it is 22.7 m/s. Obviously a smaller particle needs a higher injection velocity to penetrate into Fe-C-S smelting bath as compared to that required by a larger particle. It also shows that an increase in carbon content

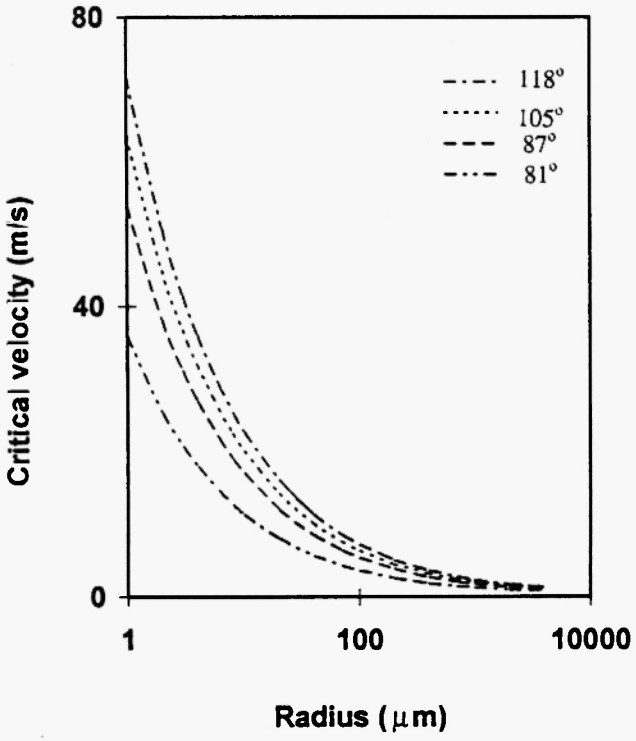

Fig. 5: The change in critical velocity with particle size for injection of carbon particle into Fe-C-Ss melt with various contact angles.

causes an increase in contact angle and subsequently leads to an increased critical velocity of engulfment. The effect of adding sulfur to carbon rich Fe-C-S melts is to deteriorate further the wettability of carbon particles and melts. This will result in an increase in critical velocity of engulfment. Under non-wetting conditions ($\theta > 90°$) an increase in θ gives rise to an increase in the value of v_c, according to equation (18). Thus large critical injection velocities are required for carbon particles of small radius to be injected in sulfur rich Fe-C-S melts. Especially for particle radii less than 100 μm, Figure 6 also shows the importance of the role played by contact angles. This implies that for the carbon particles typically employed in metallurgical processes (sizes – 10-100 μm) the contact angle could have a significant influence on injection velocity and therefore could dictate the melt/carbon interfacial area and any other subsequent reactions occurring at the interface.

5. CONCLUSIONS

In this study an equation of motion was developed

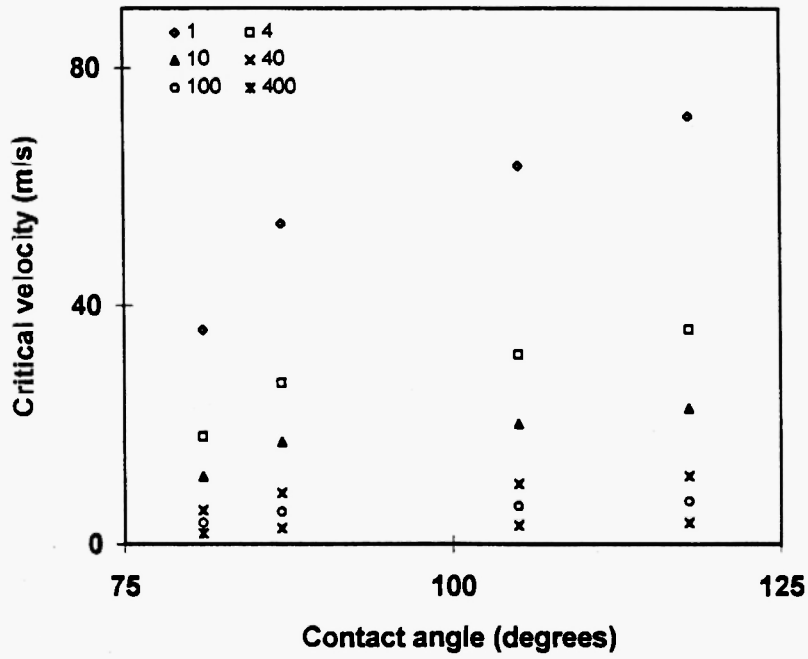

Fig. 6: The variation of critical velocity of carbon particles of different sizes in Fe-C-S melts as a function of contact angle.

for predicting the critical velocity of engulfment of a particle into melt using the force balance approach. The effect of penetration depth on buoyancy force was taken into account explicitly along with forces of gravity, surface tension, and drag. It could be seen that:

1. The critical velocities for engulfment of spheres calculated by the new model were found to be in good agreement with the available experimental data on critical entry velocity of glass, stainless steel, sapphire and Hastelloy B in a mercury bath. If buoyancy was the only force acting on the sphere, it turns out that the contribution from the whole sphere as a function of penetration depth exactly matches the contribution from the half immersed sphere. While Ozawa and Mori /8/ used this assumption without providing any justification, we have developed an exact general expression for the force balance and critical engulfment velocity.
2. For coal/slag systems, the critical velocities of carbon particle engulfment calculated from the new model by using reasonable values of contact angles were found to lie in between the maximum velocity of engulfment values derived by Siderenko's correlation and the minimum velocity derived by Voronova's correlation. The results, however, were closer to the results obtained from Voronova's correlation.
3. The critical engulfment velocity for carbon particles lies in the range 4.3 to 5.6 m/s for 100 μm particles in carbon/slag (CaO-SiO_2-Al_2O_3-MgO-Fe_2O_3) systems.
4. Engulfment of carbon particles of the same size will be more difficult in Fe-C-S melts with higher sulfur and carbon concentrations. For the carbon particles typically employed in metallurgical processes (sizes 10 –100 μm) the contact angle could have a significant influence on the critical carbon particles velocity of engulfment which will in turn dictate the melt/carbon interfacial area and subsequent reactions occurring at the interface.

NOMENCLATURE

A	empirical constant
C_D	drag coefficient
G	variable defined in Eq. (5)
T	temperature in degrees Kelvin
We	Weber number
a	variable defined in Eq. (14)
a_s	sulfur activity
K_s	coefficient used for surface tension
b	variable defined in Eq. (15)
c	variable defined in Eq. (19)
$-\frac{dv}{dt}$	deceleration
$f(x)$	function defined in Eq. (16)
g	acceleration due to gravity
r_p	particle radius
v	velocity of particle
v_0	initial velocity of the particle relative to the interface
v_c	critical velocity of penetration of particle
x	penetration depth
α	virtual mass coefficient
γ_{lv}	gas-melt interfacial tension
ρ^*	ratio of the density of the particle and the density of the liquid
ρ_l	density of melt
θ	contact angle
$\Phi(x/r_p)$	correction factor for C_D

REFERENCES

1. A. Wikander, Powdered alloys for injection, in: *Scaninject, International Conference of Injection Metallurgy*, Lulea, Sweden, 1977.
2. N. Siddiqi, V. Sahajwalla, O. Ostrovski and G.R. Belton, Wettability of graphite by CaO-SiO_2-Al_2O_3-FeO-Mg slag, accepted for publication in *High Temperature Materials and Processes*, 1997.
3. A.S. Mehta, V. Sahajwalla and J.J. Poveromo, Consumption of residual char in blast furnace during coal injection–slag/carbon/gas interactions, accepted for publication in the *Proceedings of the 56th Ironmaking Conference*, 1997.
4. M.P. Siderenko, Theory and practice of powder injection into the metal, *Metallurgiya, Moscow*, (1975).
5. N.A. Voronova, Development of some theoretical and technological aspects of blowing granular

magnesium into pig iron, *Metallurgiya, Moscow*, 237-242 (1993).

6. F. Jorgensen, F.J. Moyle and J.K. Wright, in: *Metallurgical Processes for the Early Twenty First Century*, H.Y. Sohn (ed.), The Minerals & Metals Society, 1994; pp. 321-337.
7. T.A. Engh, H. Sandberg, A. Hultkvist and L.G. Noreberg, Si de-oxidation of steel by injection of slags with low SiO_2 activity, *Scand. J. Met.*, 1, 103-114 (1972).
8. Y. Ozawa and K. Mori, Critical condition for penetration of solid particles into liquid metals, *Transactions ISIJ*, 23, 769-774 (1983).
9. R. Bird, W.E. Stewart and E.N. Lightfoot, *Transport Phenomena*, Wiley & Sons, Inc., New York, 1960; pp. 192.
10. I. Imai, *Fluid Dynamics I*, Syobako, Tokyo, 1975.
11. *Slag Atlas*, Verein Deutscher Eisenhuttenleute (Eds.), Verlag Stahleisen GmbH, Dusseldorf, 1995.
12. I. Jimbo, A. Sharan and A.W. Cramb, Recent measurements of surface and interfacial tensions in steels, in: *Steelmaking Conference Proceedings*, 1993; 485-494.